Military Technical College
Kobry El-Kobbah,
Cairo, Egypt

11th International Conference
on Electrical Engineering
ICEENG 2018

Performance evaluation of deceptive and noise jamming on SAR focused image

Mohamed E. Hanafy*, Hossam Eldin A. Hassan*, Mohamed S. Abdel-Latif*, and Sherif A. Elgamel*

ABSTRACT

Synthetic aperture radar (SAR) has been involved in military applications such as high resolution imaging, battle field surveillance, and moving target detection. Recently noise and deception jamming signal are introduced to counter SAR sensor, thus these jamming techniques can be used to protect ground targets or objects of high interest. In this paper, a comparative study of the performance of the deceptive and the noise jamming on a SAR focused image, with and without jamming, is performed. Two evaluations craterous, structural similarity index measure (SSIM), and correlation coefficient (CC) are used to measure the previous jamming techniques effect on a real SAR focused image (object of high interest). The computer based simulation results, reveal that for the same CC, the power required by the deceptive jamming is reduced by three order of magnitude compared with the power required by conventional noise jamming, mean while for the same SSIM the required power is reduced by nearly two order of magnitude.

I-Introduction

A golden age of remote sensing was started by using synthetic aperture radar (SAR), due to its amazing capabilities in operating in day and night, and in all weather conditions[1]. SAR has been involved in military applications such as high resolution imaging, battle field surveillance, and moving target detection[2]. These applications are used in capturing the focused image (object of high interest). To protect these objects, there is a need to counter SAR sensor. Generally, two jamming techniques can be used to counter SAR sensor, noise jamming, and deceptive jamming. The noise jamming techniques require a very high jamming power values[3-5]. The existing deceptive jamming techniques can generate a deceptive jamming signal for a large scene but with dividing the large scene into several sub-templates [6]. In [7],another deceptive jamming technique can generate a fast SAR deceptive jamming signal, valid for large scene, based on inverse range Doppler algorithm (IRDA), but didn't take the range cell migration phenomenon (RCM) in consideration.

* Egyptian Armed Forces

Thus, there is degradation occurs to the deceptive jamming image. The deceptive jamming signals is required to be coherent with the real SAR signal [7]. To solve the problem of generating a coherent SAR signal, the SAR signal parameters can be divided into three categories: the first category is the kinematic parameters, such as SAR platform position, and speed. The second category is the SAR antenna parameters such as antenna aperture length, number of samples in azimuth, and range. The third category is the Transmitting signal parameters, such as signal carrier frequency, and pulse repetition frequency (PRF) [8]. To obtain the previous surveillance information's, a synergy netting deception jamming is generated based on collaborative receivers, thus the performance of the deceptive jamming signal is improved [9].

In this paper, a deceptive jamming signal, of a large scene, is generated based on IRDA taking into consideration the RCM phenomenon, by introducing an inverse range cell migration correction (IRCMC) block to the algorithm of the generation process. A comparative study of the evaluation effect of additive noise jamming technique, and deceptive jamming technique on a SAR focused image is discussed at different jamming to signal ratio (JSR) values. The jamming effect on SAR is evaluated by two evaluations craterous structural similarity index measure (SSIM), and correlation coefficient (CC). The evaluation tests were performed for different JSR.

This paper is built up of five sections. Section II introduces the noise and deceptive jamming techniques against SAR, and the jamming effect evaluation craterous. The mathematical model of the deceptive jamming raw data signal is derived in section III. Section IV presents the simulation and results for the performance evaluation of deceptive and noise jamming on SAR focused image. Section V concludes the paper.

II- Jamming techniques and its evaluation effect on SAR

SAR is likely to be countered by two techniques of the electronic countermeasures (ECM) to prevent target detection and classification. First the noise jamming technique, which needs a massive power output to mask the SAR image. In practice, this technique doesn't always provide a practical ECM against the SAR [4]. Second, a more potent threat can be presented by the deceptive jamming, which can exploit the SAR processing gain and secure the sensitive sites using low power output [5]. A survey of these ECM techniques and its evaluation effect on SAR are presented in the following subsections

II-a Additive noise jamming technique

SAR has two matched filters (range, and azimuth matched filters) at its receiving system [10]. These filters add a very high level of the compression gain to the SAR return echo [10]. The jamming signal power level should exceed the value of the added compression gain, to be able to effect on SAR sensor. In this section, additive (pulsed) white Gaussian noise jamming signal is applied to the SAR. The jamming noise is a time domain, pulsed Gaussian noise, which is band limited to the radar pulse width rather than the whole pulse reputation interval (PRI). The values of the1-D noise are stored along a linear path (vector), while the values of the 2-D noise are sat on a matrix. As shown in Fig.1, the 2-D noise is then applied to a range and azimuth low path filters, to be band limited in the range and in the azimuth directions, respectively. Then, the jamming noise is directly added to the radar signal in an incoherent way, at the radar receiver input. For this jamming technique the jamming signal is given by [11]

$$j(t,s) = n(t,s), \tag{1}$$

where $j(t,s)$is the noise jamming signal, $n(t,s)$is a 2-D conventional white Gaussian noise.The input to the SAR $x(t)$can be written as:

$$x(t) = s_r(t,s) + j(t,s) \quad (2)$$

where $s_r(t,s)$is the SAR return echo signal. The deceptive jamming technique will be discussed in the following section.

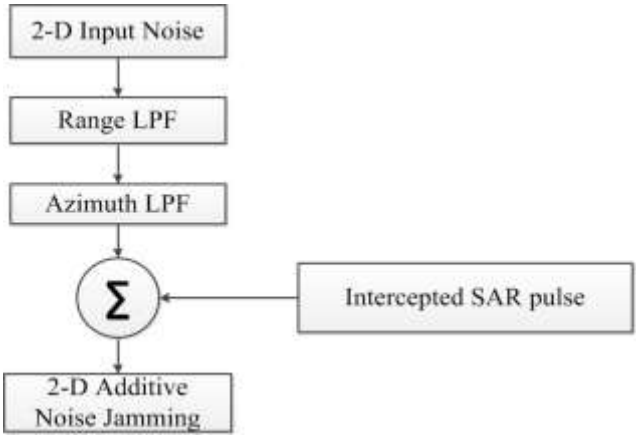

Fig.1: Generation of the additive jamming noise

II-b Deceptive jamming technique

The deceptive jamming principle on SAR depends on introducing a spurious scene or target on its image. The deceptive jamming signal should have the same (Kinematic, antenna, and signal) parameters of the SAR return echo, from the protected area. Assuming that the SAR flies in a straight path and subjected to the geometric parameters, as shown in Fig.2. The jammer lies inside the protected area, the beam of the jammer has a slant angle (θ_j).

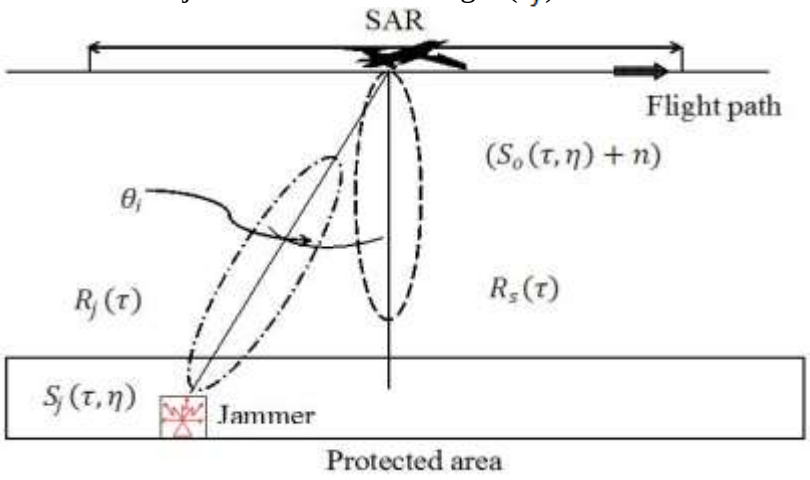

Fig.2: Geographic relationship of the SAR radar platform towards the jammer

Next section is going to discuss the effect evaluation craterous of the jamming techniques

II-c Jamming effect evaluation craterous

The jamming effect is evaluated by two creatures SSIM and CC. The SSIM is applied as a quantitative method for estimating the perceived quality of the digital images of the SAR. The SSIM algorithm can give a prediction of image quality, based on the initial distortion to a reference image. The reference image is the jamming free image of the SAR sensor. Assuming x is the SAR reference image, and y is the image with jamming. The structural similarity index between the two images $SSIM(x,y)$ is given by[12]:

$$SSIM(x,y) = \frac{(2\mu_x\mu_y+c_1)(2\sigma_{xy}+c_2)}{(\mu_x{}^2+\mu_y{}^2+c_1)(\sigma_x{}^2+\sigma_y{}^2+c_2)}, \quad (3)$$

where, μ_x and μ_y are the mean values of intensities of x and y, respectively. σ_X and σ_Y, are the standard deviation of x and y respectively. σ_{xy}, is the correlation coefficient between (*x, y*), and c_1, and c_2 are constants to avoid instability.

The correlation coefficient, CC, can reflect the statistical relativity of two images. Let *x* and *y* are two images, without, and with jamming respectively, such that $X = \{x(f_i,g_j)\}_{i=0,j=0}^{m,n}$, and $Y = \{y(f_i,g_j)\}_{i=0,j=0}^{m,n}$, for SAR. The CC between them can be represented by [13].

$$\rho_{FG} = \frac{\sum_{j=0}^{n}\sum_{i=0}^{m} x(f_i,g_j)gx_i,y_j)}{[\sum_{j=0}^{n}\sum_{i=0}^{m} x(f_i,g_j)^2 * \sum_{j=0}^{n}\sum_{i=0}^{m} y(f_i,g_j)^2]^{1/2}}, \quad (4)$$

The deceptive jamming signal from a point target $s_j(\tau,\eta)$ can be expressed by[10]:

$$s_j(\tau,\eta) = A_j\, w_r(\tau - \frac{2R_j(\eta)}{c}) w_a(\eta-\eta_c) \times \exp\{-j4\pi f_o \frac{R_j(\eta)}{c}\} \times exp\{j\pi K_r(\tau - \frac{2R_j(\eta)}{c})^2\}\ , \quad (5)$$

where A_j is an arbitrary complex constant, $w_r(\tau)$ is the range envelope (a rectangular function), τ is the range time,$R_j(\eta)$is the Instantaneous jammer slant range, c is the speed of the light,$w_a(\eta)$ is the azimuth envelope (a sinc squared function),η is the azimuth time referenced to closest approach, $\eta_c$is the beam center offset time, $f_o$is the radar center frequency, and$K_r$is the range chirp FM rate.

III- Modeling of SAR deceptive jamming signal.

The IRDA performs two decompression processes to generate the SAR deceptive jamming signal, azimuth and range decompression, respectively. The azimuth decompression is performed by multiplying the azimuth decompression filter in each azimuth column of the signal. Similarly, the range decompression process can be made by multiplying the range decompression filter in each range column of the signal, as illustrated in Fig.3. The generated signal from a spurious scene or a synthesized image $s_{si}(\eta,\tau)$ can be given by:

$$s_{si}(\eta,\tau) = A_j P_r(\tau - \frac{2R_{jo}}{c}) P_a(\eta)\, exp\left\{-j\frac{4\pi f_o R_{jo}}{c}\right\} exp\{j2\pi f_{\eta c}\eta\}, \quad (6)$$

where $P_r(\tau)$ is the compressed pulse envelope, $P_a(\eta)$ is the amplitude of the impulse response of the azimuth, R_{jo} is the jammer slant range of the closest approach.

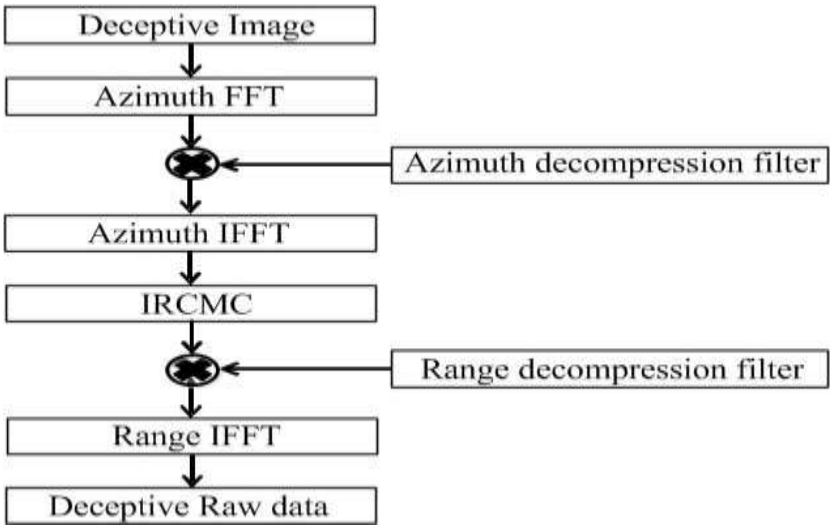

Fig.3: Deceptive jamming signal generation based on IRDA

This signal is transformed into frequency domain in the azimuth direction, which can be expressed by:

$$S_{si}(\tau, f_\eta) = FFT_\eta\left(s_{si}(\eta, \tau)\right). \\ = A_j P_r\left[\tau - \frac{2R_0}{c}\right] W_a(f_\eta - f_{\eta c}) \exp\left\{-j\frac{4\pi f_o R_{jo}}{c}\right\}, \quad (7)$$

where $FFT_\eta\left(s_{si}(\eta, \tau)\right)$ is the fast Fourier transform of the signal in the azimuth direction, f_η is the azimuth frequency, $f_{\eta c}$ is the beam offset frequency. The response of the azimuth decompression filter is given by:

$$H_{azdc}(f_\eta) = exp\{j\pi\frac{f_\eta^2}{K_a}\}, \quad (8)$$

where $K_a = \frac{2v_r^2}{\lambda R_{jo}}$.

The output of the azimuth decompression filter is computed as:

$$S_{azdc}(\eta, f_\eta) = S_{si}(\tau, f_\eta).H_{azdc}(f_\eta) \quad (9)$$

By substituting from (7), (8) into (9), the azimuth decompressed signal can be expressed as:

$$S_{azdc}(\eta, f_\eta) = A_j P_r\left[\tau - \frac{2R_0}{c}\right] W_a(f_\eta - f_{\eta c}) \times exp\left\{-j\frac{4\pi f_o R_{jo}}{c}\right\} exp\{j\pi\frac{f_\eta^2}{K_a}\}, \quad (10)$$

The response of the IRCMC is given by the following [10]

$$G_{ircmc}(f_\tau) = exp\{-j\frac{4\pi f_\tau \Delta R_j(f_\eta)}{c}\}, \quad (11)$$

where, $\Delta R_j(f_\eta) = \frac{\lambda^2 R_{jo} f_\eta^2}{8v_r^2}$.

Thus, the output of the IRCMC is given by:

$$S_{ircmc}(\tau, f_\eta) = S_{azdc}(\eta, f_\eta).G_{ircmc}(f_\tau).$$

$$= A_j P_r \left[\tau - \frac{2R_0}{c}\right] W_a(f_\eta - f_{\eta c}) \times exp\left\{-j\frac{4\pi f_o R_o}{c}\right\} exp\{j\pi \frac{f_\eta^2}{K_a}\} exp\{-j\frac{4\pi f_\tau \Delta R_j(f_\eta)}{c}\} \quad . \quad (12)$$

The signal is then transformed into frequency domain in range direction, which can be expressed as following:

$$S_{ircmc}(f_\tau, f_\eta) = FFT_\tau\left(s_{ircmc}(\tau, f_\eta)\right) \quad (13)$$

The range decompression filter is expressed in range frequency domain by:

$$H_{rdc}(f_\tau) = exp\{-j\pi f_\tau^2\left(\frac{1}{K_r} - \frac{1}{K_{src}(R_{jo}, f_\eta)}\right), \quad (14)$$

where $K_{src}(R_o, f_\eta) = \frac{2v_r^2 f_o^2 D^3(f_\eta, v_r)}{cR_{jo} f_\eta^2}$.

The output of the range decompression filter is calculated by:

$$S_{rdc}(f_\tau, f_\eta) = \{S_{ircmc}(f_\tau, f_\eta) H_{rdc}(f_\tau)\}. \quad (15)$$

The required deceptive jamming raw data signal is obtained by performing an inverse fast Fourier transform (*IFFT*) in both azimuth and range dimensions on the output of the range decompression filter, as following

$$s_j(\tau,\eta) = IFFT_{\tau,\eta}\ (S_{rdc}(f_\tau, f_\eta))$$

$$s_j(\tau,\eta) = A_j\, w_r\left(\tau - \frac{2R_j(\eta)}{c}\right) w_a(\eta - \eta_c) \times exp\left\{-j4\pi f_o \frac{R_j(\eta)}{c}\right\} \times exp\{j\pi K_r(\tau - \frac{2R_j(\eta)}{c})^2\}, \quad (16)$$

For the jammer has a slant angle θ_j, then$R_j(\eta) = \sqrt{R_{jo}^2 + v^2\eta^2 - 2R_{jo}v\eta sin\theta_j}$

The SAR return echo can be given by:

$$s_o(\tau,\eta) = A_r w_r\left(\tau - \frac{2R_s(\eta)}{c}\right) w_a(\eta - \eta_c) \times \exp\left\{-j4\pi f_o \frac{R_s(\eta)}{c}\right\} \times \quad \exp\{j\pi K_r\left(\tau - \frac{2R_s(\eta)}{c}\right)^2\}\} + n(\tau,\eta) \quad (17)$$

,

where $A_r$is the arbitrary complex constant related to the SAR return echo, $n(\tau,\eta)$is the SAR internal noise. The received signal at the front end of the SAR is given by

$$s_{rec}(\tau,\eta) = s_j(\tau,\eta) + \left(s_o(\tau,\eta) + n(\tau,\eta)\right), \quad (18)$$

By substituting from (14), (15) into (16), the received signal can be given by

$$s_{rec}(\tau,\eta) = A_j\, w_r(\tau - \frac{2R_j(\eta)}{c}) w_a(\eta - \eta_c) \times \exp\{-j4\pi f_o \frac{R_j(\eta)}{c}\} \times exp\{j\pi K_r\left(\tau - \frac{2R_j(\eta)}{c}\right)^2 + A_r\, w_r(\tau - \frac{2R_s(\eta)}{c}) w_a(\eta - \eta_c) \times \exp\left\{-j4\pi f_o \frac{R_s(\eta)}{c}\right\} \times \quad \exp\{j\pi K_r(\tau - \frac{2R_s(\eta)}{c})^2\} + n \quad (19)$$

,

If the jammer is coincident with the protected object ($\theta_j = 0$), so$R_s(\eta) = R_j(\eta) = \sqrt{R_{jo}^2 + v^2\eta^2}$, and the received signal can be given by:

$$s_{rec}(\tau,\eta) = (A_j + A_r)[w_r\left(\tau - \frac{2R_j(\eta)}{c}\right) w_a(\eta - \eta_c) \times \exp\{-j4\pi f_o \frac{R_j(\eta)}{c}\} \times exp\{j\pi K_r(\tau - \frac{2R_j(\eta)}{c})^2\}] + n(\tau,\eta) \quad (20)$$

.

This formula is used in the simulation of the received signal at the SAR receiver front end in section IV.

IV - Simulation and results

In the simulation, SAR is considered to work in strip-map mode, and its platform flies in a straight path. The SAR parameters are listed in Table I.

Table I: SAR parameters

Parameter	**Value**
Carrier Frequency	35 GHZ
Propagation speed (*C*)	3×10^8
Chirp pulse duration	1µsec
Transmitted Bandwidth	1 MHZ
A/D Sampling rate	250 MHZ
Pulse repetition frequency (*PRF*)	1 KHZ
Effective antenna dimension along azimuth direction (*La*)	0.5 m
Effective antenna dimension along range direction (*Lr*)	0.2 m
SAR platform moving speed	56 m/sec
Radar High	1.4 km

Fig.4 shows the real SAR image of Washington DC which is required to be protected. It was captured by Sandia National Laboratory KU-Band SAR, which is carried by the Sandia Twin Otter aircraft. The input image to the IRDA algorithm, as shown in Fig.5, is subjected to two decompression processes. The input image will be converted to a raw data with number of samples in azimuth (*Na*) =1650samples, and number of samples in range (*Nr*) = 2778 samples, as shown in Fig.6. All the jamming study were performed in a signal to noise ratio (SNR) value of SAR =12 dB, using (17).

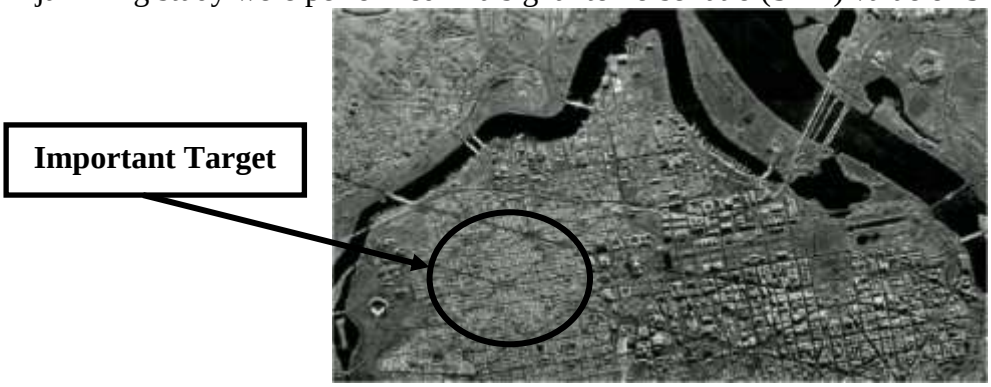

Fig.4 SAR real image of Washington DC

Fig.5 The input Image

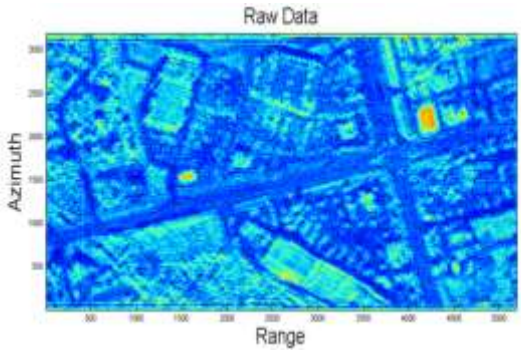

Fig.6 The generated raw data

Fig.7 shows the simulation process of the jamming scenario, and the evaluation of the jamming effect. The SAR signal is first intercepted, and its (Kinematic, antenna, and signal) parameters are considered to be estimated by the ESM part of the jamming station. The jamming signal is added to the SAR signal in two cases. Firstly, the 2-D noise jamming signal is generated with the same size of the SAR signal. The power level of the JSR is controlled with ranges from (0 dB to 40 dB), using (2), as this level range can give the same performance of that level range of the deceptive jamming. The signal is added to the SAR return echo at the SAR receiver front end.

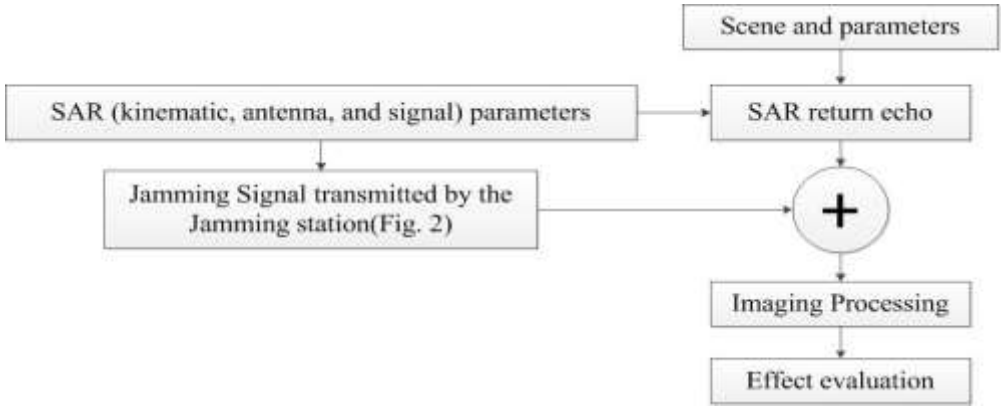

Fig.7 Deceptive jamming scenario and its evaluation effect

Secondly, the deceptive jamming raw data signal is modified with the SAR parameters listed in Table I. For the purpose of simulation, the signal power of the SAR return echo is normalized to 0dB. The deceptive jamming signal is transmitted with different values of signal power ratio, ranges from (-10 dB to 10 dB), using (20), thus the JSR value is controlled.

Both SSIM and the CC values range from zero to one. So if that value becomes smaller, that means that the jammed image is more different from the original one. In other words the jamming effect is much better. As shown in Table II, the SSIM, and the CC becomes smaller with the increase of JSR. In Fig.8-a, using (4), the correlation coefficient reaches 0.8389 at JSR = 0dB, and CC reaches 0.5721 at JSR = 35 dB of noise jamming, as in Fig.8-b. However nearly theses values can be obtained in deceptive jamming at JSR = -5 dB, and at JSR = 3 dB, using (3), as shown in Fig.8-c and Fig.8-d. The SSIM value becomes 0.3152 at JSR = 28 dB of noise jamming, where in the deceptive jamming this value becomes 0.3118 at JSR = 10 dB, it is evident that the humane vision can't extract information from the SAR image when its SSIM value is equal to or less than 0.3[12]. Fig.9-a shows the SAR focused image under noise jamming at JSR = 28 dB, Fig.9-b shows the SSIM maps and value (0.3152)

of SAR focused image under noise jamming of JSR = 28 dB, Fig.9-c shows the SAR image under deceptive jamming of JSR = 10 dB, Fig.9-d shows the SSIM maps and value (0.3118) of SAR image under deceptive jamming of JSR = 10, these two SSIM values are nearly the same.

Table II: Evaluation effect of noise and deceptive jamming

The evaluation effect of noise jamming			The evaluation effect of deceptive jamming		
JSR	CC	SSIM	JSR	CC	SSIM
No Jam	1	1	**No Jam**	1	1
0	0.8389	0.4126	**-10**	0.9245	07927
10	0.8377	0.4108	**-9**	0.9132	0.7731
20	0.8256	0.3926	**-7**	0.8854	0.7302
23	0.8126	0.3745	**-5**	0.8484	0.6834
25	0.7981	0.3558	**-3**	0.8003	0.6325
27	0.7762	0.3304	**0**	0.7061	0.5528
28	0.7616	0.3152	**3**	0.5912	0.4720
29	0.7445	0.2985	**5**	0.5105	0.4209
30	0.7241	0.2808	**7**	0.4327	0.3734
35	0.5721	0.1856	**9**	0.3617	0.3309
40	0.3547	0.1098	**10**	0.3296	0.3118

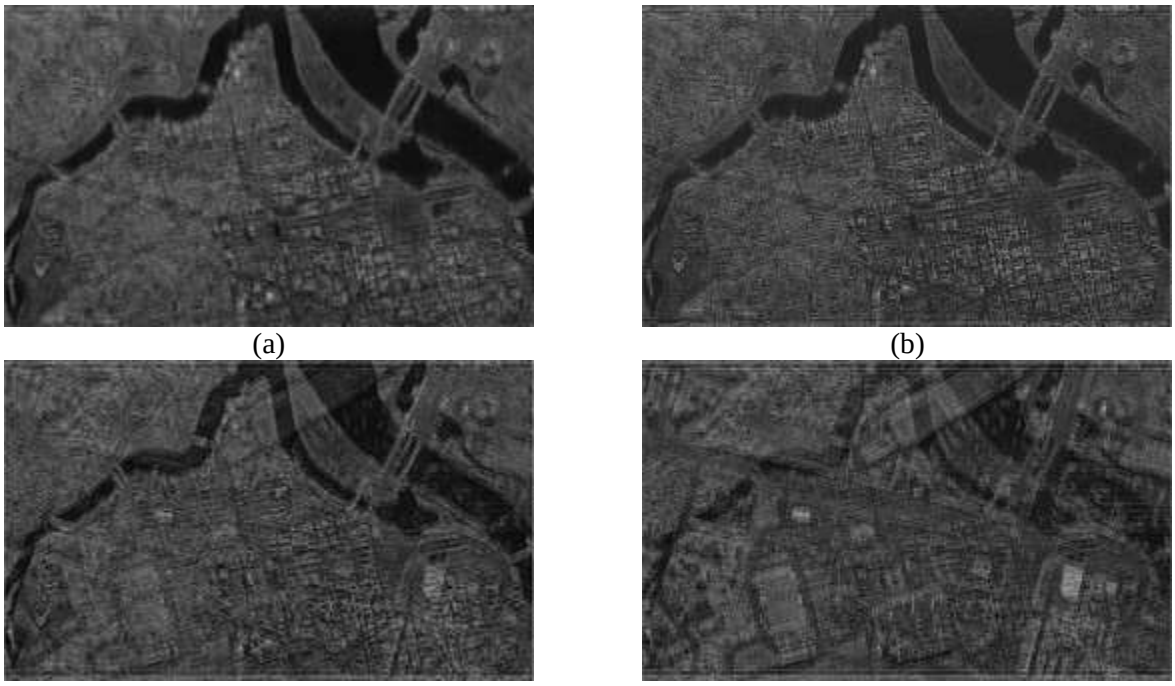

(a) (b) (c) (d)

Fig.8 Performance evaluation of SAR image under jamming techniques using CC.
(a) SAR image under noise jamming of JSR = 0 dB.
(b) SAR image under noise jamming of JSR=35 dB.
(c) SAR image under deceptive jamming of JSR= -5 dB.
(d) SAR image under deceptive jamming of JSR= 3 dB.

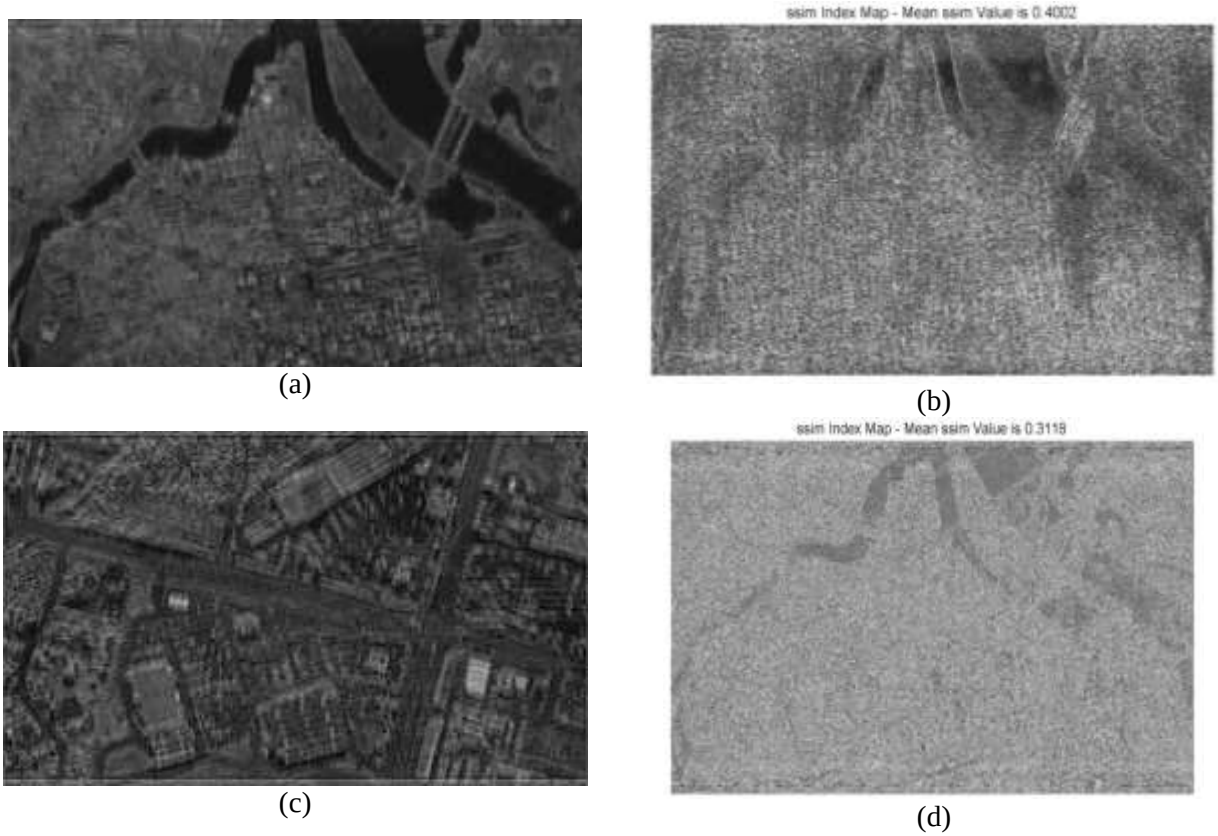

Fig.9 Performance evaluation of SAR image under jamming techniques using SSIM.
(a) SAR image under noise jamming at JSR = 28 dB.
(b) SSIM map and value of 0.3152 under noise jamming at JSR = 28 dB.
(c) SAR image under deceptive jamming at JSR = 10 dB.
(d) SSIM map and value of 0.3118 under deceptive jamming at JSR = 10 dB.

Conclusion

This paper discusses the generation of a coherent deceptive jamming signal based on IRDA. In addition, the jamming effect on the SAR under both noise, and deceptive jamming signal was studied. A comparative study of SAR performance under different values of JSR of both noise and deceptive jamming techniques are also introduced in this paper. The results emphasizes on the massive noise power required to counter SAR from capturing the important targets, which reaches up to 40 dB. However the results reveal the surprising low level of the deceptive jamming signal, at JSR=10 dB to obtain nearly the same results using the CC evaluation criteria. Moreover the required value of JSR of the noise jamming signal reaches to 28 dB to have the same SSIM of 10 dB of deceptive jamming signal.

References

[1] H. Breit, *et al.*, "TerraSAR-X SAR Processing and Products," *IEEE Transactions on Geoscience and Remote Sensing*, vol. 48, pp. 727-740, 2010.

[2] S. Brusch, *et al.*, "Ship Surveillance With TerraSAR-X," *IEEE Transactions on Geoscience and Remote Sensing*, vol. 49, pp. 1092-1103, 2011.

[3] M. A. Ammar, *et al.*, "Performance evaluation of SAR in presence of multiplicative noise jamming," in *2017 34th National Radio Science Conference (NRSC)*, 2017, pp. 213-220.
[4] Y. Lee, *et al.*, "A study on jamming performance evaluation of noise and deception jammer against SAR satellite," in *2011 3rd International Asia-Pacific Conference on Synthetic Aperture Radar (APSAR)*, 2011, pp. 1-3.
[5] R. S. Harness and M. C. Budge, "A study on SAR noise jamming and false target insertion," in *IEEE SOUTHEASTCON 2014*, 2014, pp. 1-8.
[6] F. Zhou, *et al.*, "A Large Scene Deceptive Jamming Method for Space-Borne SAR," *IEEE Transactions on Geoscience and Remote Sensing*, vol. 51, pp. 4486-4495, 2013.
[7] X. Lin, *et al.*, "Fast generation Of SAR deceptive jamming signal based on inverse Range Doppler algorithm," in *IET International Radar Conference 2013*, 2013, pp. 1-4.
[8] Y. Liu, *et al.*, "Influence of Estimate Error of Radar Kinematic Parameter on Deceptive Jamming Against SAR," *IEEE Sensors Journal*, vol. 16, pp. 5904-5911, 2016.
[9] B. Zhao, *et al.*, "Performance Improvement of Deception Jamming Against SAR Based on Minimum Condition Number," *IEEE Journal of Selected Topics in Applied Earth Observations and Remote Sensing*, vol. 10, pp. 1039-1055, 2017.
[10] I. G. Cumming and F. H. Wong, "Digital processing of synthetic aperture radar data."
[11] L. Bo, "Simulation study of noise convolution jamming countering to SAR," in *2010 International Conference On Computer Design and Applications*, 2010, pp. V4-130-V4-133.
[12] S. Jiao and W. Dong, "SAR Image Quality Assessment Based on SSIM Using Textural Feature," in *2013 Seventh International Conference on Image and Graphics*, 2013, pp. 281-286.
[13] S. Long, *et al.*, "Research on deceptive jamming technologies against SAR," in *2009 2nd Asian-Pacific Conference on Synthetic Aperture Radar*, 2009, pp. 521-525.